8-21-2015

Ground-Based Transit Observations Of The HAT-P-18, HAT-P-19, HAT-P-27/WASP40 And WASP-21 Systems

M. Seeliger

M. Kitze

R. Errmann

See next page for additional authors

Recommended Citation

M. Seeliger et al. (2015). "Ground-Based Transit Observations Of The HAT-P-18, HAT-P-19, HAT-P-27/WASP40 And WASP-21 Systems". *Monthly Notices Of The Royal Astronomical Society*. Volume 451, Issue 4. 4060-4072. DOI: 10.1093/mnras/stv1187
https://works.swarthmore.edu/fac-physics/269

Monthly Notices of the ROYAL ASTRONOMICAL SOCIETY
MNRAS **451,** 4060–4072 (2015) doi:10.1093/mnras/stv1187

Ground-based transit observations of the HAT-P-18, HAT-P-19, HAT-P-27/WASP40 and WASP-21 systems

M. Seeliger,[1⋆] M. Kitze,[1] R. Errmann,[1,2] S. Richter,[1] J. M. Ohlert,[3,4] W. P. Chen,[5] J. K. Guo,[5] E. Göğüş,[6] T. Güver,[7] B. Aydın,[6] S. Mottola,[8] S. Hellmich,[8] M. Fernandez,[9] F. J. Aceituno,[9] D. Dimitrov,[10] D. Kjurkchieva,[11] E. Jensen,[12] D. Cohen,[12] E. Kundra,[13] T. Pribulla,[13] M. Vaňko,[13] J. Budaj,[13,14] M. Mallonn,[15] Z.-Y. Wu,[16] X. Zhou,[16] St. Raetz,[1,17] C. Adam,[1] T. O. B. Schmidt,[1,18] A. Ide,[1] M. Mugrauer,[1] L. Marschall,[19] M. Hackstein,[20] R. Chini,[20,21] M. Haas,[20] T. Ak,[7] E. Güzel,[22] A. Özdönmez,[23] C. Ginski,[1,24] C. Marka,[1] J. G. Schmidt,[1] B. Dincel,[1] K. Werner,[1] A. Dathe,[1] J. Greif,[1] V. Wolf,[1] S. Buder,[1] A. Pannicke,[1] D. Puchalski[25] and R. Neuhäuser[1]

Affiliations are listed at the end of the paper

Accepted 2015 May 22. Received 2015 May 21; in original form 2014 October 7

ABSTRACT

As part of our ongoing effort to investigate transit timing variations (TTVs) of known exoplanets, we monitored transits of the four exoplanets HAT-P-18b, HAT-P-19b, HAT-P-27b/WASP-40b and WASP-21b. All of them are suspected to show TTVs due to the known properties of their host systems based on the respective discovery papers. During the past three years 46 transit observations were carried out, mostly using telescopes of the Young Exoplanet Transit Initiative. The analyses are used to refine the systems' orbital parameters. In all cases we found no hints for significant TTVs, or changes in the system parameters inclination, fractional stellar radius and planet-to-star radius ratio. However, comparing our results with those available in the literature shows that we can confirm the already published values.

Key words: planets and satellites: individual: HAT-P-18b – planets and satellites: individual: HAT-P-19b – planets and satellites: individual: HAT-P-27b/WASP-40b – planets and satellites: individual: WASP-21b.

1 INTRODUCTION

Observing extrasolar planets transiting their host stars has become an important tool for planet detection and is used to obtain and constrain fundamental system parameters: The inclination has to be close to 90°, while the planet-to-star radius ratio is constrained mainly by the transit depth. Also, in combination with spectroscopy, the semimajor axis and the absolute planet and star radii can be obtained.

Several years ago, when the first results of the *Kepler* mission were published (see Borucki et al. 2011 for first scientific results and Koch et al. 2010 for an instrument description), studying the transit timing became one of the standard techniques in the analysis of transit observations. Commonly the mid-time of each transit observation is plotted into an observed minus calculated (O−C) diagram (Ford & Holman 2007), where the difference between the observed transit mid-time and the mid-time obtained using the initial ephemeris is shown versus the observing epoch. In such a diagram, remaining slopes indicate a wrong orbital period, while e.g. periodic deviations from a linear trend indicate perturbing forces. Since space-based missions are able to observe many consecutive transit events with high precision, one can detect even small variations of the transit intervals indicating deviations from a strictly Keplerian motion and thus yet hidden planets in the observed system. Furthermore, with the discovery of multiplanetary systems, transit timing variations (TTVs) are used to find the mass of the companions without the need of radial velocity (RV) measurements due to the influence of planetary interaction on TTVs. Since many planet candidates found in photometric surveys are too faint for RV follow-up even with bigger telescopes, TTV analyses can be considered as a photometric workaround to estimate masses.

Although the existence of TTVs can be shown in already known exoplanetary systems, only a few additional planet candidates have

⋆ E-mail: martin.seeliger@uni-jena.de

Table 1. The observing telescopes that gathered data within the TTV project for HAT-P-18b, HAT-P-19b, HAT-P-27b/WASP-40b and WASP-21b in order of the number of observed transit events of the Observatory. The table lists the telescopes and corresponding observatories, as well as the telescope diameters ⌀ and number of observed transit events per telescope in this project $N_{\rm tr}$.

#	Observatory	Telescope (abbreviation)	⌀(*m*)	$N_{\rm tr}$
1	Michael Adrian Observatory Trebur (Germany)	T1T (Trebur 1.2 m)	1.2	8
2	Graduate Institute of Astronomy Lulin (Taiwan & USA)	Tenagra II (Tenagra 0.8 m)	0.8	5
		RCOS16 (Lulin 0.4 m)	0.4	2
3	University Observatory Jena (Germany)	90/60 Schmidt (Jena 0.6 m)	0.9/0.6	5
		Cassegrain (Jena 0.25 m)	0.25	3
4	TÜBİTAK National Observatory (Turkey)	T100 (Antalya 1.0 m)	1.0	5
5	Calar Alto Astronomical Observatory (Spain)	1.23 m Telescope (CA-DLR 1.2 m)	1.23	4
6	Sierra Nevada Observatory (Spain)	Ritchey-Chrétien (OSN 1.5 m)	1.5	2
7	Peter van de Kamp Observatory Swarthmore (USA)	RCOS (Swarthmore 0.6 m)	0.6	2
8	National Astronomical Observatory Rozhen (Bulgaria)	Ritchey-Chrétien-Coudé (Rozhen 2.0 m)	2.0	1
		Cassegrain (Rozhen 0.6 m)	0.6	1
9	Teide Observatory, Canarian Islands (Spain)	STELLA-I (Stella 1.2 m)	1.2	2
10	University Observatory Bochum (Cerro Armazones, Chile)	VYSOS6 (Chile 0.15 m)	0.15	1
11	Xinglong Observing Station (China)	90/60 Schmidt (Xinglong 0.6 m)	0.9/0.6	1
12	Gettysburg College Observatory (USA)	Cassegrain (Gettysburg 0.4 m)	0.4	1
13	Stará Lesná Observatory (Slovak Rep.)	0.5 m Reflector (StaraLesna 0.5 m)	0.5	1
14	Istanbul University Telescope at Çanakkale (Turkey)	0.6 m Telescope (Çanakkale 0.6 m)	0.6	1
15	Toruń Centre for Astronomy (Poland)	0.6 m Cassegrain Telescope (Torún 0.6 m)	0.6	1

been found using TTVs so far. One of the most prominent examples is the KOI-142 system. By analysing the TTV signals of KOI-142b, Mazeh et al. (2013) suggested the existence of additional planets in the system. Later on, Nesvorný et al. (2013) proposed a non-transiting planet KOI-142c that was confirmed using RV measurements by Barros et al. (2014). Regarding ground-based analyses e.g. Maciejewski et al. (2011a) and von Essen (2013) found indications of TTVs potentially induced by additional planets. The lack of confirmed TTV planets is not surprising, since large bodies often can be found using RV measurements or direct transit detections, while small (e.g. Earth-like) objects result in small TTV amplitudes and therefore high-precision timing measurements are needed. However, these measurements can already be acquired with medium size ground-based telescopes.

Besides the discovery of small planets, the amount of known massive planets on close-in orbits increased as well. First studies on a larger sample of planet candidates detected with *Kepler* suggest that hot giant planets exist in single planet systems only (Steffen et al. 2012). However, Szabó et al. (2013) analysed a larger sample of *Kepler* hot Jupiters and found a few cases where TTVs cannot be explained by other causes (e.g. artificial sampling effects due to the observing cadence) but the existence of perturbers – additional planets or even exomoons – in the respective system. In addition, Szabó et al. (2013) point towards the planet candidates KOI-338, KOI-94 and KOI-1241, who are all hot Jupiters in multiplanetary systems, as well as the WASP-12 system with a proposed companion candidate found by ground-based TTV analysis (Maciejewski et al. 2011a).

The origin of those planets is yet not fully understood. One possible formation scenario shows that close-in giant planets could have migrated inwards after their creation further out (Steffen et al. 2012). In that case, inner and close outer planets would have either been thrown out of the system, or caught in resonance. In the latter case, even small perturbing masses, e.g. Earth-mass objects, can result in TTV amplitudes in the order of several minutes (see Ford & Holman 2007 or Seeliger et al. 2014). Though *Kepler* is surveying many of those systems, it is necessary to look at the most promising candidates among all close-in giant planets discovered so far. Since many of the stars observed with *Kepler* are too faint to perform RV follow-up, investigating stars outside the field of view (FoV) of *Kepler*, e.g. objects found by HATnet (Bakos et al. 2004) or the WASP project (Pollacco et al. 2006), is advisable. In our ongoing study[1] of TTVs in exoplanetary systems we perform photometric follow-up observations of specific promising transiting planets where additional bodies are expected. The targets are selected by the following criteria.

(i) There is an indication for a perturber in the system, e.g. a non-zero eccentricity in the orbital solution of the known transiting planet (though the circularization time-scale is much shorter than the system age) or deviant RV data points.

(ii) The brightness of the host star is $V \leq 13$ mag and the transit depth is at least 10 mmag to ensure sufficient photometric and timing precision at 1–2 m class ground-based telescopes.

(iii) The target is visible from the Northern hemisphere.

(iv) The target has not been studied for TTV signals before.

In the past the transiting exoplanets WASP-12b (Maciejewski et al. 2011a, 2013b), WASP-3b (Maciejewski et al. 2010, 2013a), WASP-10b (Maciejewski et al. 2011b; Maciejewski et al., in preparation) , WASP-14b (Raetz 2012; Raetz et al. 2015), TrES-2 (Raetz et al. 2014) and HAT-P-32b (Seeliger et al. 2014) have been studied by our group in detail. In most cases, except for WASP-12b, no TTVs could be confirmed.

Here, we extend our investigations to search for TTVs in the HAT-P-18, HAT-P-19, HAT-P-27/WASP-40 and WASP-21 planetary systems. In Section 2, we give a short description of the targets analysed within this project. Section 3 explains the principles of data acquisition and reduction and gives an overview of the telescopes used for observation. The modelling procedures are described in Section 4, followed by the results in Section 5. Finally, Section 6 gives a summary of our project.

[1] see http://ttv.astri.umk.pl/doku.php for a project overview.

Table 2. The list of all transit observations gathered within the TTV project sorted by object and date. Though no pre-selections for quality or completeness have been applied to this list, transits used for further analysis have been marked by an asterisk. The filter subscripts B, C and J denote the photometric systems of Bessel, Cousins and Johnson, respectively. The last column lists the number of exposures and the exposure time of each observation.

#	Date	Telescope	Filter	Exposures
		HAT-P-18b		
1*	2011-04-21	Trebur 1.2 m	R_B	189 × 90 s
2	2011-05-02	Trebur 1.2 m	R_B	123 × 45 s
3*	2011-05-24	Trebur 1.2 m	R_B	323 × 60 s
4	2011-06-04	Rozhen 2.0 m	R_C	1000 × 10 s
5*	2012-05-05	Rozhen 0.6 m	I_C	219 × 90 s
6	2012-06-07	CA DLR 1.23 m	B_J	250 × 60 s
7	2013-04-28	Antalya 1.0 m	R	214 × 50 s
8	2014-03-30	Toruń 0.6 m	Clear	297 × 40 s
		HAT-P-19b		
9*	2011-11-23	Jena 0.6 m	R_B	246 × 50 s
10	2011-11-23	Jena 0.25 m	R_B	320 × 50 s
11	2011-11-23	Trebur 1.2 m	R_B	461 × 30 s
12	2011-12-05	Jena 0.6 m	R_B	129 × 60 s
13	2011-12-05	Jena 0.25 m	V_B	28 × 300 s
14*	2011-12-09	Jena 0.6 m	R_B	290 × 50 s
15	2011-12-09	Jena 0.25 m	V_B	118 × 150 s
16	2011-12-09	Trebur 1.2 m	R_B	380 × 35 s
17*	2011-12-17	CA DLR 1.23 m	R_J	273 × 60 s
18	2014-08-01	Antalya 1.0 m	R	148 × 60 s
19	2014-08-05	Antalya 1.0 m	R	196 × 40 s
20	2014-08-21	Jena 0.6 m	R_B	152 × 50 s
21*	2014-10-04	Jena 0.6 m	R_B	280 × 50 s
		HAT-P-27b		
22*	2011-04-05	Lulin 0.4 m	R_B	166 × 40 s
23*	2011-04-08	Lulin 0.4 m	R_B	250 × 40 s
24	2011-05-03	Stella 1.2 m	Hα	180 × 100 s
25*	2011-05-05	Trebur 1.2 m	R_B	162 × 70 s
26	2011-05-08	Stella 1.2 m	Hα	190 × 100 s
27	2011-05-21	Tenagra 0.8 m	R	141 × 40 s
28	2012-03-07	StaraLesna 0.5 m	R	361 × 30 s
29	2012-03-29	Tenagra 0.8 m	R	240 × 30 s
30	2012-04-01	Tenagra 0.8 m	R	329 × 20 s
31	2012-04-04	Tenagra 0.8 m	R	333 × 20 s
32	2012-04-25	Xinglong 0.6 m	R	154 × 40 s
33	2012-05-16	Trebur 1.2 m	R_B	231 × 70 s
34	2012-05-25	Chile 0.15 m	I_J/R_J	220 × 80 s
35	2012-06-13	Tenagra 0.8 m	R	223 × 15 s
36*	2013-06-03	Antalya 1.0 m	R	156 × 60 s
37*	2013-06-03	OSN 1.5 m	R	435 × 30 s
38	2013-06-06	CA DLR 1.23 m	R_J	172 × 60 s
39*	2014-06-18	Antalya 1.0 m	R	146 × 50 s
		WASP-21b		
40*	2011-08-24	Swarthmore 0.6 m	R_B	545 × 45 s
41	2011-08-24	Gettysburg 0.4 m	R	230 × 60 s
42*	2012-08-16	Trebur 1.2 m	R_B	365 × 40 s
43	2012-10-20	Antalya 1.0 m	R	242 × 40 s
44*	2013-09-18	CA DLR 1.23 m	R_J	584 × 30 s
45	2013-09-22	Antalya 1.0 m	R	208 × 50 s
46	2013-09-22	Ulupinar 0.6 m	R_B	163 × 110 s

2 TARGETS

2.1 HAT-P-18b and HAT-P-19b

Hartman et al. (2011) reported on the discovery of the exoplanets HAT-P-18b and HAT-P-19b. The two Saturn-mass planets orbit their early K-type host stars with periods of 5.51 and 4.01 d, respectively.

In the case of HAT-P-18b, Hartman et al. (2011) found the eccentricity to be slightly non-zero ($e = 0.084 \pm 0.048$). Recent studies of Esposito et al. (2014) found the eccentricity to be consistent with a non-eccentric retrograde orbit by analysing the Rossiter–McLaughlin effect. Knutson et al. (2014) also analysed the RV signal and found a jitter of the order of 17.5 m s^{-1} that remains unexplained. Ginski et al. (2012) presented the results of the lucky imaging campaign with AstraLux at the Calar Alto 2.2 m Telescope to search for additional low-mass stellar companions in the system. With the data gathered in this previous study objects down to a mass of $0.140 \pm 0.022\,M_\odot$ at angular separations as small as 0.5 arcsec and objects down to $0.099 \pm 0.008\,M_\odot$ outside of 2 arcsec could already be excluded. In addition to this study, we performed follow-up observations of HAT-P-18b planetary transits, as well as a monitoring project of the planet host star over a longer time span to possibly find overall brightness variations.

For HAT-P-19b, a small eccentricity of $e = 0.067 \pm 0.042$ was determined by Hartman et al. (2011). They also found a linear trend in the RV residuals pointing towards the existence of a long-period perturber in the system. Within this project we want to address the problem of the proposed perturber using photometric methods, i.e. follow-up transit events to find planetary induced TTV signals.

2.2 HAT-P-27b/WASP-40b

HAT-P-27b (Béky et al. 2011), independently discovered as WASP-40b by Anderson et al. (2011) within the WASP-survey (Pollacco et al. 2006), is a typical hot Jupiter with a period of 3.04 d. While the eccentricity was found to be $e = 0.078 \pm 0.047$ by Béky et al. (2011), Anderson et al. (2011) adopted a non-eccentric orbit. However, the latter authors found a huge spread in the RV data with up to 40 m s^{-1} deviation from the circular single planet solution. According to Anderson et al. (2011) one possible explanation, despite a changing activity of the K-type host star, is the existence of a perturber that might not be seen in the Béky et al. (2011) data due to the limited data set. However, the authors suggest further monitoring to clarify the nature of the system. One possibility is to study the companion hypothesis from the TTV point of view.

Another interesting aspect is the transit shape of HAT-P-27b. With an increasing impact parameter $b = a/R_s \cos i$, the typical flat bottom phase of the box-shaped transit becomes shorter and even vanished completely for grazing transit events (V-shaped transit). The data of Béky et al. (2011) show a flat bottom phase, while the best-fitting solutions of Anderson et al. (2011) and Sada et al. (2012) point towards a V-shape. The latter ones found that there is a high probability that the system is grazing using the grazing criterion (Smalley et al. 2011). Though this would explain the unusual shape of the transit, the impact parameter of the U-shaped transit seen by Béky et al. (2011) ($b = 0.89$) lies between the one derived by Anderson et al. (2011) and Sada et al. (2012) ($b = 0.86$ and $b = 0.92$, respectively). New high-quality observations of HAT-P-27b planetary transits could be used to further constrain the real system configuration.

Table 3. The input parameters for the JKTEBOP and TAP runs for all objects listed in Section 2. All values have been obtained from the original discovery papers. LD coefficients are taken from Claret & Bloemen (2011) linear interpolated in terms of $T_{\rm eff}$, log g and [Fe/H] using the EXOFAST/QUADLD code (Eastman et al. 2013). Free parameters are marked by an asterisk. At the bottom the duration of ingress and egress according to Winn (2010) has been added.

Object	HAT-P-18b	HAT-P-19b	HAT-P-27b	WASP-21b
$r_{\rm p} + r_{\rm s}$*	0.0575(19)	0.0709(33)	0.1159(65)	0.0959(44)
$R_{\rm p}/R_{\rm s}$*	0.1365(15)	0.1418(20)	0.1186(31)	0.1040(35)
i (°)*	88.8(3)	88.2(4)	84.7(7)	88.75(84)
$a/R_{\rm s}$*	16.04(75)	12.24(67)	9.65(54)	10.54(48)
$M_{\rm p}/M_{\rm s}$	0.000 243(26)	0.000 329(37)	0.000 663(58)	0.000 282(19)
e	0.084(48)	0.067(42)	0.078(47)	0
P (d)	5.508 0023(06)	4.008 778(06)	3.039 586(12)	4.322 482(24)
R (mag)	12.61	12.82	11.98	11.52
$T_{\rm eff}$ (K)	4803(80)	4990(130)	5300(90)	5800(100)
log g (cgs)	4.57(04)	4.54(05)	4.51(04)	4.2(1)
[Fe/H] (dex)	+0.10(08)	+0.23(08)	+0.29(10)	−0.46(11)
$v \sin i$ (km s^{-1})	0.5(5)	0.7(5)	0.4(4)	1.5(6)
LD law of the star	Quadratic	Quadratic	Quadratic	Quadratic
R band linear*	0.5736	0.5433	0.4808	0.3228
R band non-linear*	0.1474	0.1710	0.2128	0.2982
V band linear*	0.7180	0.6783	0.6002	0.4055
V band non-linear*	0.0697	0.1039	0.1643	0.2892
$\tau_{\rm egress/ingress}$ (min)	22.8	23.1	37.8	20.1

2.3 WASP-21b

The planetary host star WASP-21, with its Saturn-mass planet on a 4.32 d orbit discovered by Bouchy et al. (2010), is one the most metal-poor planet hosts accompanied by one of the least dense planets discovered by ground-based transit searches to date. Bouchy et al. (2010) found that including a small non-zero eccentricity to the fit does not improve the results. Hence, they concluded that the eccentricity is consistent with zero.

In a later study, Barros et al. (2011) found the G3V star to be in the process of moving off the main sequence. Hence, though the WASP-21 system does not match our criteria concerning the expectations for additional bodies in the system, we included further observations of WASP-21b planetary transits to improve the knowledge on this system.

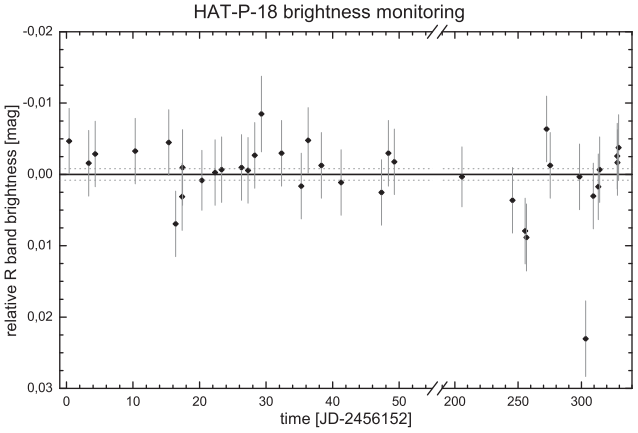

Figure 1. Relative R-band brightness of the star HAT-P-18 over a time span of 12 months. The dotted line represents the rms of a constant fit.

3 DATA ACQUISITION AND REDUCTION

Our observations make use of YETI network telescopes (Young Exoplanet Transit Initiative; Neuhäuser et al. 2011), a worldwide network of small- to medium-size telescopes mostly on the Northern hemisphere established to explore transiting planets in young open clusters.

A summary of all participating telescopes and the number of performed observations can be found in Table 1. Most of the observing telescopes are part of the YETI network. This includes telescopes at Cerro Armazones (Chile, operated by the University of Bochum), Gettysburg (USA), Jena (Germany), Lulin (Taiwan), Rozhen (Bulgaria), Sierra Nevada (Spain), Stará Lesná (Slovak Republic), Swarthmore (USA), Tenagra (USA, operated by the National Central University of Taiwan) and Xinglong (China). For details about location, mirror and chip, see Neuhäuser et al. (2011).

In addition to the contribution of the YETI telescopes, we obtained data using the following telescopes:

(i) the 1.2 m telescope of the German–Spanish Astronomical Center on Calar Alto (Spain), which is operated by German Aerospace Center (DLR);

(ii) the 1.2 m robotic telescope STELLA-I, situated at Teide Observatory on Tenerife (Spain) and operated by the Leibnitz-Institut für Astrophysik Potsdam;

(iii) the Trebur 1 Meter Telescope operated at the Michael Adrian Observatory Trebur (Germany);

(iv) the T100 telescope of the TÜBITAK National Observatory (Turkey);

(v) the 0.6 m telescope (CIST60) at Ulupınar Observatory operated by Istanbul University (Turkey);

(vi) the 0.6 m Cassegrain telescope of the Toruń Centre for Astronomy (Poland).

Besides the transit observations, the Jena 0.6 m telescope with its Schmidt Teleskop Kamera (Mugrauer & Berthold 2010) was used to perform a long term monitoring of HAT-P-18 as described in Sections 2.1 and 5.1.

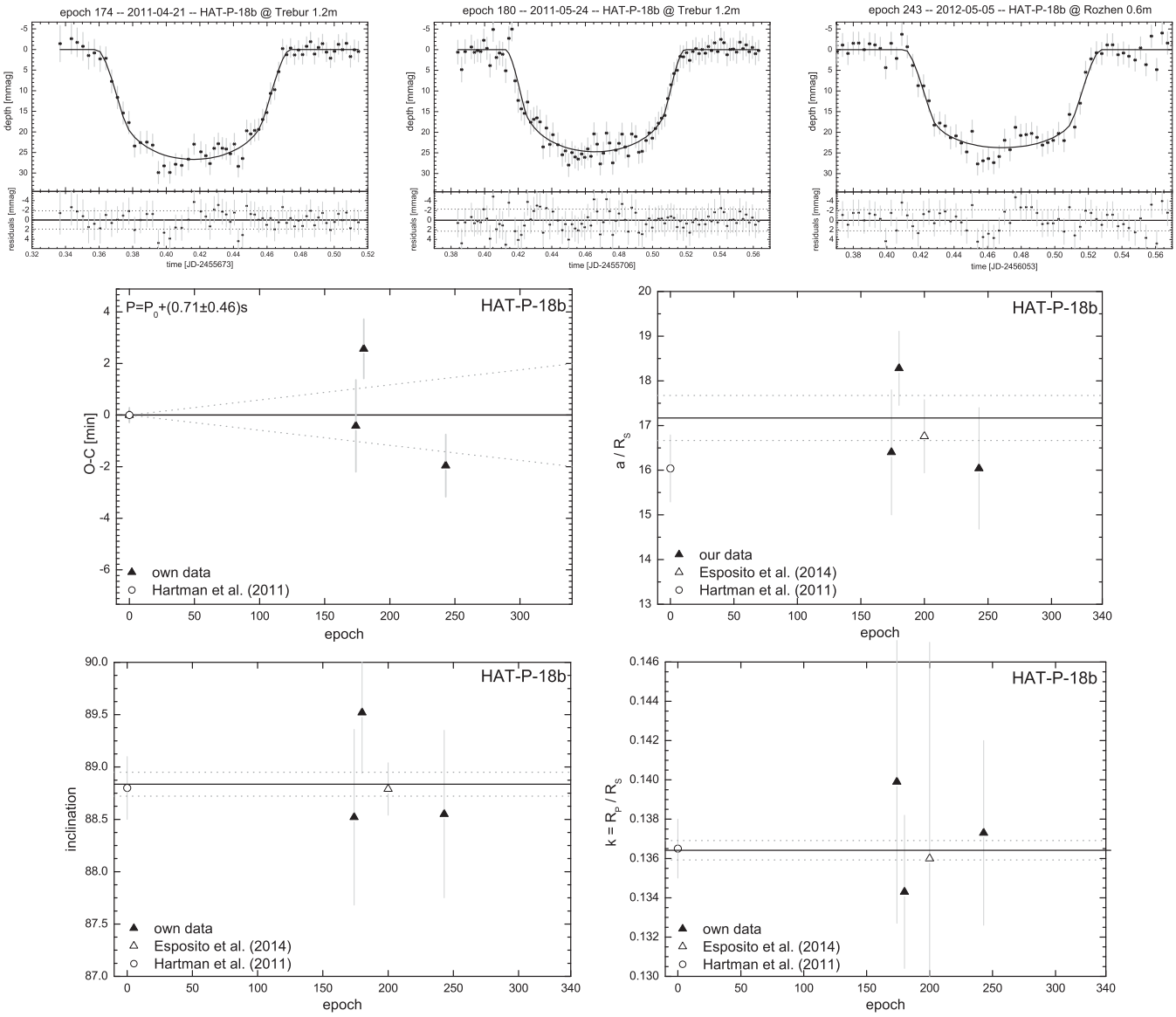

Figure 2. Top: the threefold binned transit light curves of the three complete transit observations of HAT-P-18b. The upper panels show the light curve, the lower panels show the residuals. The rms of the fit of the threefold binned light curves (dotted lines) are shown as well. Bottom: the present result for the HAT-P-18b observing campaign, including the O−C diagram, as well as the results for the reverse fractional stellar radius a/R_s, the inclination i and the planet-to-star radius ratio k. The open circle denotes literature data from Hartman et al. (2011) and the open triangles denote data from Esposito et al. (2014). Filled triangles denote our data (from Trebur and Rozhen). The dotted line shows the 1σ error bar of the constant fit .

Between 2011 April and 2013 June our group observed 46 transit events (see Table 2) using 18 different telescopes (see Table 1). 16 observations could be used for further analysis, while 30 observations had to be rejected due to several reasons, e.g. no full transit event has been observed or bad weather conditions and hence low signal to noise. For example, Southworth et al. (2009a, 2009b) showed that defocusing the telescope allows us to reduce flat fielding effects. Since the light of a star is spread over a larger amount of pixels and more light is gathered due to a longer exposure time, seeing effects are reduced as well as photon noise. Since a defocused image spreads the light over several CCD pixel, one can increase the exposure time and hence the effective duty cycle of the CCD assuming a constant read out time (as mentioned also in the conclusions of Barros et al. 2011). Thus we tried to defocus the telescope and increase the exposure time during all our observations. Table 3 lists the ingress/egress durations τ derived using the formulas (18) and (19) given in Winn (2010). With our strategy we obtain at least one data point within 90 s. This ensures to have at least 10 data points during ingress/egress phase which is required to fit the transit model to the data and get precise transit mid-times.

All data have been reduced in a standard way by applying dark/bias and flat-field corrections using IRAF.[2] The respective calibration images have been obtained in the same night and

[2] IRAF is distributed by the National Optical Astronomy Observatories, which are operated by the Association of Universities for Research in Astronomy, Inc., under cooperative agreement with the National Science Foundation.

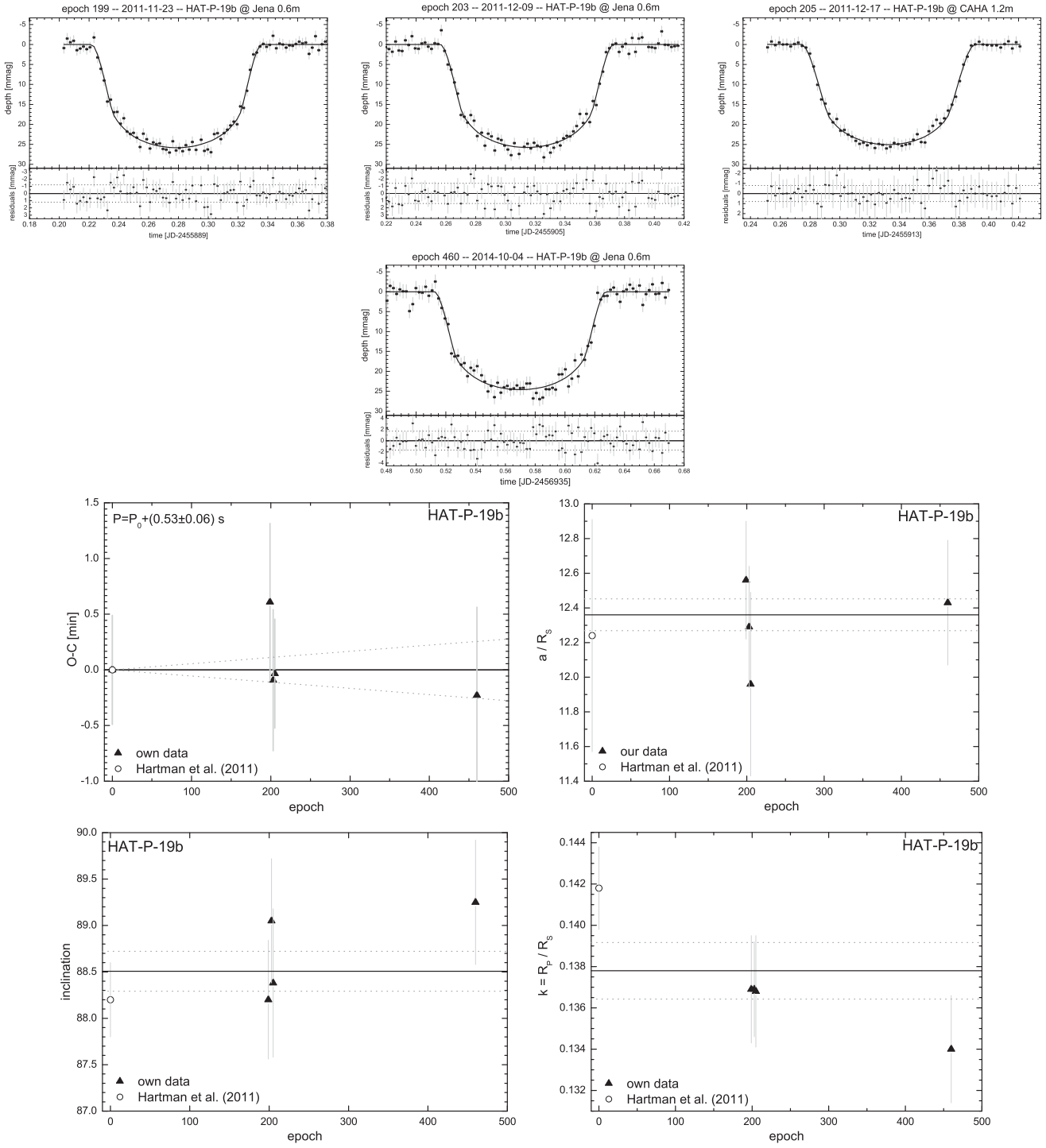

Figure 3. Top: the transit light curves obtained for HAT-P-19b. Bottom: the present result for the HAT-P-19b observing campaign. All explanations are equal to Fig. 2. The open circle denotes literature data from Hartman et al. (2011) and filled triangles denote our data (from Jena and Calar Alto).

with the same focus as the scientific observations. This is necessary especially if the pointing of the telescope is not stable. When using calibration images obtained with different foci, patterns remain in the images that lead to distortions in the light curve.

Besides our own observations, we also use literature data. This involves data from the respective discovery papers mentioned in Section 2, as well as data from Esposito et al. (2014) in the case of HAT-P-18b, Sada et al. (2012) in the case of HAT-P-27b, Barros et al. (2011) and Ciceri et al. (2013) for WASP-21b, and Simpson et al. (2010) for WASP-38b.

4 ANALYSES

The light-curve extraction and modelling is performed analogous to the procedure described in detail in Seeliger et al. (2014).

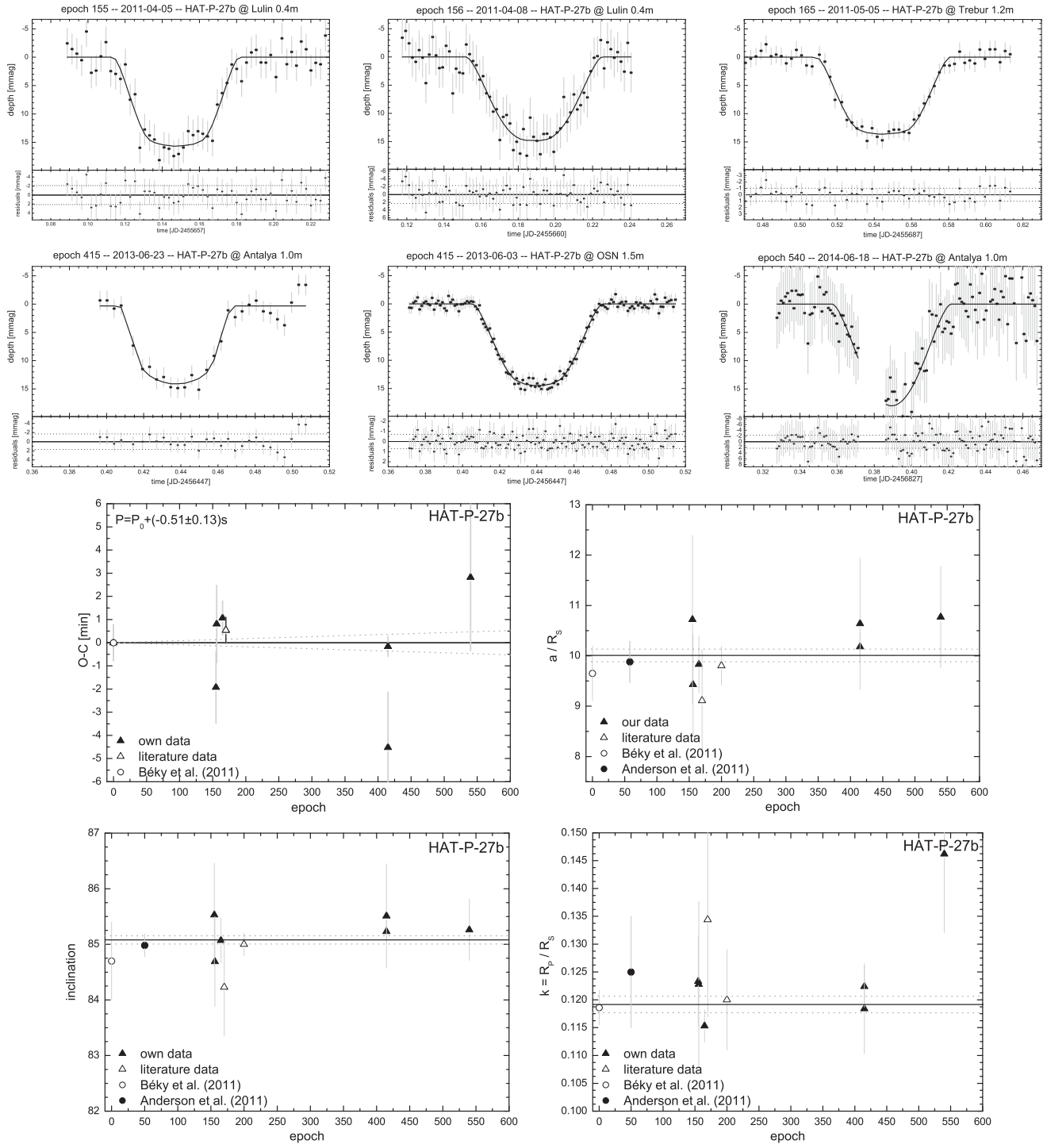

Figure 4. Top: the transit light curves obtained for HAT-P-27b. Bottom: the present result for the HAT-P-27b observing campaign. All explanations are equal to Fig. 2. The open circles denote data from the discovery papers of Béky et al. (2011) and Anderson et al. (2011), open triangles denote literature data from Sada et al. (2012) and Brown et al. (2012) (the latter one set to epoch 200 artificially), filled triangles denote our data (from Lulin, Trebur, Xinglong and Antalya).

4.1 Light-curve extraction

The Julian date of each image is calculated from the header information of the start of the exposure and the exposure time. To precisely determine the mid-time of the transit event, these pieces of information have to be stored most accurate. The reliability of the final light-curve model thus also depends on a precise time synchronization of the telescope computer system. Since all data are obtained using JD_{UTC} as time base, we transform the fitted mid-transit times to BJD_{TDB} afterwards using the online converter[3] provided by

[3] http://astroutils.astronomy.ohio-state.edu/time/utc2bjd.html

Table 4. Impact parameters of HAT-P-27b planetary transits.

Observation epoch	Impact parameter
155 – Lulin 0.4 m	0.84 ± 0.30
156 – Lulin 0.4 m	0.87 ± 0.23
165 – Trebur 1.2 m	0.84 ± 0.12
415 – Antalya 1.0 m	0.81 ± 0.27
415 – OSN 1.5 m	0.85 ± 0.06
540 – Antalya 1.0 m	0.89 ± 0.19
Our analysis combined	0.859 ± 0.023
Béky et al. (2011)	0.89 ± 0.17
Anderson et al. (2011)	0.86 ± 0.07
Sada et al. (2012)	0.92 ± 0.24
Brown et al. (2012)	0.85 ± 0.07

Jason Eastman (for a detailed description of the barycentric dynamical time see Eastman, Siverd & Gaudi 2010).

We use differential aperture photometry to extract the light curve from the reduced images by measuring the brightness of all bright stars in the field with routines provided by IRAF. The typical aperture radius is ≈1.5 times the mean full width half-maximum of all stars in the FoV. The best-fitting aperture is found by manually varying the aperture radius by a few pixels to minimize the photometric scatter. The final light curve is created by comparing the star of interest against an artificial standard star composed of the (typically 15–30) brightest stars in the FoV weighted by their respective constantness as introduced by Broeg, Fernández & Neuhäuser (2005).

The final photometric errors are based on the instrumental IRAF measurement errors. The error of the constant comparison stars are rescaled by their photometric scatter using shared scaling factors in order to achieve a mean $\chi^2_{\rm red} \approx 1$ for all comparison stars. The error bars of the transit star are rescaled afterwards using the same scaling factors (for further details on the procedure, see Broeg et al. 2005).

Trends in light curves induced by atmospheric effects can impact the determination of transit parameters. To eliminate such effects we start the observation about 1 h before and finish about 1 h after the transit itself. Thus we can detrend the observations by fitting a second-order polynomial to the out-of-transit data.

4.2 Modelling with TAP and JKTEBOP

To model the light curves we used the Transit Analysis Package (TAP, version v2.104; Gazak et al. 2012). The modelling of the transit light curve is done by using the EXOFAST routines (Eastman, Gaudi & Agol 2013) with the light-curve model of Mandel & Agol (2002). For error estimation TAP uses Markov Chain Monte Carlo simulations (in our case 10 times 10^5 MCMC chains) together with wavelet-based likelihood functions (Carter & Winn 2009). The coefficients for the quadratic limb-darkening (LD) law used by TAP are taken from the EXOFAST/QUADLD-routine of Eastman et al. (2013)[4] that linearly interpolates the LD tables of Claret & Bloemen (2011).

For comparison we also use JKTEBOP (version 25, see Southworth 2008, and references therein) which is based on the EBOP code for eclipsing binaries (Etzel 1981; Popper & Etzel 1981). To compare the results with those obtained with TAP, we only use a quadratic LD law which is sufficient for ground-based data. For error estimation we used Monte Carlo simulations (task #7, 10^4 runs), bootstrapping (task #8, 10^4 data sets) and a residual shift method (task #9) as provided by JKTEBOP.

As input values for the modelling we take the system properties presented in the respective discovery papers (see Table 3 for a summary). As free parameters we use the mid-transit time $T_{\rm mid}$, inclination i, and planet-to-star radius ratio $k = r_{\rm p}/r_{\rm s}$ (with $r_{\rm p}$ and $r_{\rm s}$ being the planet and stellar radius scaled by the semimajor axis, respectively). In the case of TAP, the inverse fractional stellar radius $a/R_{\rm s} = 1/r_{\rm s}$, in the case of JKTEBOP the sum of the fractional radii $(r_{\rm p} + r_{\rm s})$ is fitted as well. Both quantities are an expression of the transit duration and can be transformed into each other according to the following equation:

$$a/R_{\rm s} = \left(1 + r_{\rm p}/r_{\rm s}\right) / \left(r_{\rm p} + r_{\rm s}\right) .$$

The fitting procedure is applied two times. First, keeping the LD coefficients fixed at their theoretical values, and afterwards letting them vary. For TAP we set the fitting interval to ±0.2. In the case of JKTEBOP, we use the option to set the LD coefficients fixed for the initial model, but let them being perturbed for the error estimation. Thus the fitted model does not change, but the error bars are increased. The eccentricity was fixed to zero for all our analyses.

Finally, we derive the photometric noise rate (pnr; Fulton et al. 2011) as a quality marker for all light curves, which is defined as the ratio between the root mean square of the model fit and the number of data points per minute. For further analysis, we took data with pnr $\lesssim$4.5 into account which corresponds to a timing precision of $\Delta T_{\rm mid} \approx 90$ s.

5 RESULTS

For every light curve, we get three different models, two from TAP (for the model with the LD coefficients fixed and free, respectively) and one from JKTEBOP (LD coefficients set free for error estimation only). To get one final result for every transit event, we averaged those three results. As for the errors, we got two different estimations from TAP and six from JKTEBOP. As final error value, we took the maximum of either the largest of the error estimates, or the spread of the model fit results to use a conservative error estimate. It has to be noted, though, that the spread between the different models has always been below size of the error bars.

The same counts for the differences between the TAP models obtained with fixed LD values and those obtained with the LD coefficients set free to fit. For a detailed discussion of the influence of the LD model on transit light curves, see e.g. Raetz et al. (2014).

The redetermination of the system parameters is performed with ORIGIN 6.0 (OriginLab, Northampton, MA). In order to find possible deviations from a constant value, we use the internally provided linear fitting function with a fixed slope of zero on all single results obtained for a given target and property. The individual model errors are taken as instrumental weights during the χ^2-minimization fitting procedure.

5.1 HAT-P-18b

Over a timespan of 12 months, we obtained three images in four bands (B, V, R, I) in each clear night using the Jena 0.6 m telescope in order to look at the long-term variability of the parent star. As shown in Fig. 1, the mean variation of the R-band brightness is ≈0.9 mmag taking the individual error bar of the measurements into account. The result is in agreement with no variation.

[4] The LD calculator is available online at http://astroutils.astronomy.ohio-state.edu/exofast/limbdark.shtml.

Table 5. A comparison between the results obtained in Our analysis and the literature data. All epochs T_0 are converted to BJD_{TDB}.

	$T_0\,(d)$	$P\,(d)$	a/R_s	$k = R_p/R_s$	$i\,(^\circ)$
		HAT-P-18b			
Our analysis	2454 715.022 54 ± 0.000 39	5.508 0291 ± 0.000 0042	17.09 ± 0.71	0.1362 ± 0.0011	88.79 ± 0.21
Hartman et al. (2011)	2454 715.022 51 ± 0.000 20	5.508 023 ± 0.000 006	16.04 ± 0.75	0.1365 ± 0.0015	88.3 ± 0.3
Esposito et al. (2014)	2455 706.7 ± 0.7	5.507 978 ± 0.000 043	16.76 ± 0.82	0.136 ± 0.011	88.79 ± 0.25
		HAT-P-19b			
Our analysis	2455 091.535 00 ± 0.000 15	4.008 7842 ± 0.000 0007	12.36 ± 0.09	0.1378 ± 0.0014	88.51 ± 0.22
Hartman et al. (2011)	2455 091.534 94 ± 0.000 34	4.008 778 ± 0.000 006	12.24 ± 0.67	0.1418 ± 0.0020	88.2 ± 0.4
		HAT-P-27b			
Our analysis	2455 186.019 91 ± 0.000 44	3.039 5803 ± 0.000 0015	10.01 ± 0.13	0.1192 ± 0.0015	85.08 ± 0.07
Béky et al. (2011)	2455 186.019 55 ± 0.000 54	3.039 486 ± 0.000 012	$9.65^{+0.54}_{-0.40}$	0.1186 ± 0.0031	$84.7^{+0.7}_{-0.4}$
Anderson et al. (2011)	2455 368.394 76 ± 0.000 18	3.039 5721 ± 0.000 0078	9.88 ± 0.39	0.1250 ± 0.0015	$84.98^{+0.20}_{-0.14}$
Sada et al. (2012)	2455 186.198 22 ± 0.000 32	3.039 5824 ± 0.000 0035	$9.11^{+0.71}_{-1.01}$	$0.1344^{+0.0174}_{-0.0389}$	84.23 ± 0.88
Brown et al. (2012)	–	3.039 577 ± 0.000 006	$9.80^{+0.38}_{-0.29}$	$0.120^{+0.009}_{-0.007}$	85.0 ± 0.2
		WASP-21b			
Our analysis	2454 743.042 17 ± 0.000 65	4.322 5126 ± 0.000 0022	9.62 ± 0.17	0.1030 ± 0.0008	87.12 ± 0.24
Bouchy et al. (2010)	2454 743.0426 ± 0.0022	$4.322\,482^{+0.000\,024}_{-0.000\,019}$	10.54 ± 0.49	$0.1040^{+0.0017}_{-0.0018}$	$88.75^{+0.70}_{-0.84}$
Barros et al. (2011)	2455 084.520 48 ± 0.000 20	4.322 5060 ± 0.000 0031	$9.68^{+0.30}_{-0.19}$	$0.1071^{+0.0009}_{-0.0008}$	87.34 ± 0.29
Ciceri et al. (2013)	2454 743.040 54 ± 0.000 71	4.322 5186 ± 0.000 0030	9.46 ± 0.27	0.1055 ± 0.0023	86.97 ± 0.33
Southworth (2012)	2455 084.520 40 ± 0.000 16	4.322 5060 ± 0.000 0031	9.35 ± 0.34	0.1095 ± 0.0013	86.77 ± 0.45

Looking at the Exoplanet Transit Database (ETD; Poddaný, Brát & Pejcha 2010) one can see that the values for the transit depth reported there vary by several tens of mmag. Such variations can be caused by close variable stellar companions placed within the aperture due to the pixel scale of the detectors and the telescope defocusing. However, our results together with the data of Hartman et al. (2011) and Esposito et al. (2014) neither show a variation in the transit depth, i.e. the k-value, nor the overall stellar brightness. Thus, the data provided by ETD in the case of HAT-P-27b should be treated with caution.

For HAT-P-18b, we obtained three useful transit observations (see Fig. 2). However, due to the size of the used telescopes, the relatively faint planet host star and the small amount of suitable comparison stars available in the respective FoV of each observation, the resultant light curves are dominated by a large scatter.

Except for one – but not significant – outlier the differences in the O−C diagram (see Fig. 2) can be explained by redetermining the published period by (0.53 ± 0.36) s. Hence, our result is in good agreement with the originally published period of Hartman et al. (2011).

Despite a spread in the data, which can be explained by the quality of the light curves, we do not see any significant differences for k, i and a/R_s between the respective observations. A summary of all obtained parameters can be found in Table 5, as well as a comparison with literature values.

5.2 HAT-P-19b

For HAT-P-19b, we got two light curves using the Jena 0.6 m and one light curve from the CAHA 1.2 m telescope (Fig. 3). In all three cases, we obtained high-precision data. The light curves show no artefacts that could be ascribed to e.g. spots on the stellar surface. Plotting the mid-transit times into the O−C diagram, we can redetermine the period by (0.53 ± 0.06) s. As for the inclination and the reverse fractional stellar radius, we can confirm the values reported in Hartman et al. (2011). The radius ratio of $k = 0.1378 \pm 0.0014$, however, seems to be smaller than assumed by Hartman et al. (2011) ($k = 0.1418 \pm 0.0020$).

5.3 HAT-P-27b

HAT-P-27b planetary transits were observed six times (see Fig. 4). Unfortunately, due to the observing conditions and sizes of the telescopes used for the observations most light curves are of lower quality. An advantage of a network such as the YETI network lies within the possibility of simultaneous observations using different telescopes. This enables us to independently check whether the data are reliable. For HAT-P-27b, simultaneous observations could be achieved at epoch 415 using two different telescopes (Antalya 1.0 m and OSN 1.5 m).

In addition to our own data, we added data from Sada et al. (2012) and Brown et al. (2012). The latter one only lists system parameters without giving an epoch of observation, thus we artificially put them to epoch 200. The system parameters i, a/R_s and k can be determined more precisely than before taking the errors of the individual measurements into account. All three parameters are in good agreement with the results of previous authors. Furthermore, we do not see any significant variation. The larger k-value of the epoch 540 observations are due to the quality of the corresponding light curve.

Looking at the mid-transit time we see that a period change of (−0.51 ± 0.12) s explains the data quite well. The mid-transit time of one of the epoch 415 observations was found to be ≈4.5 min ahead of time, while the other one is as predicted. This way we could identify a synchronization error during one of the observations. This example shows the importance of simultaneous transit observations. Unfortunately, this was the only successful observation of that kind within this project (for a larger set of double and threefold observations, see e.g. Seeliger et al. 2014).

As mentioned before, one of the previous discussions in the case of HAT-P-27b planetary transits has been the transit shape. Table 4 lists the derived impact parameters for our single observations,

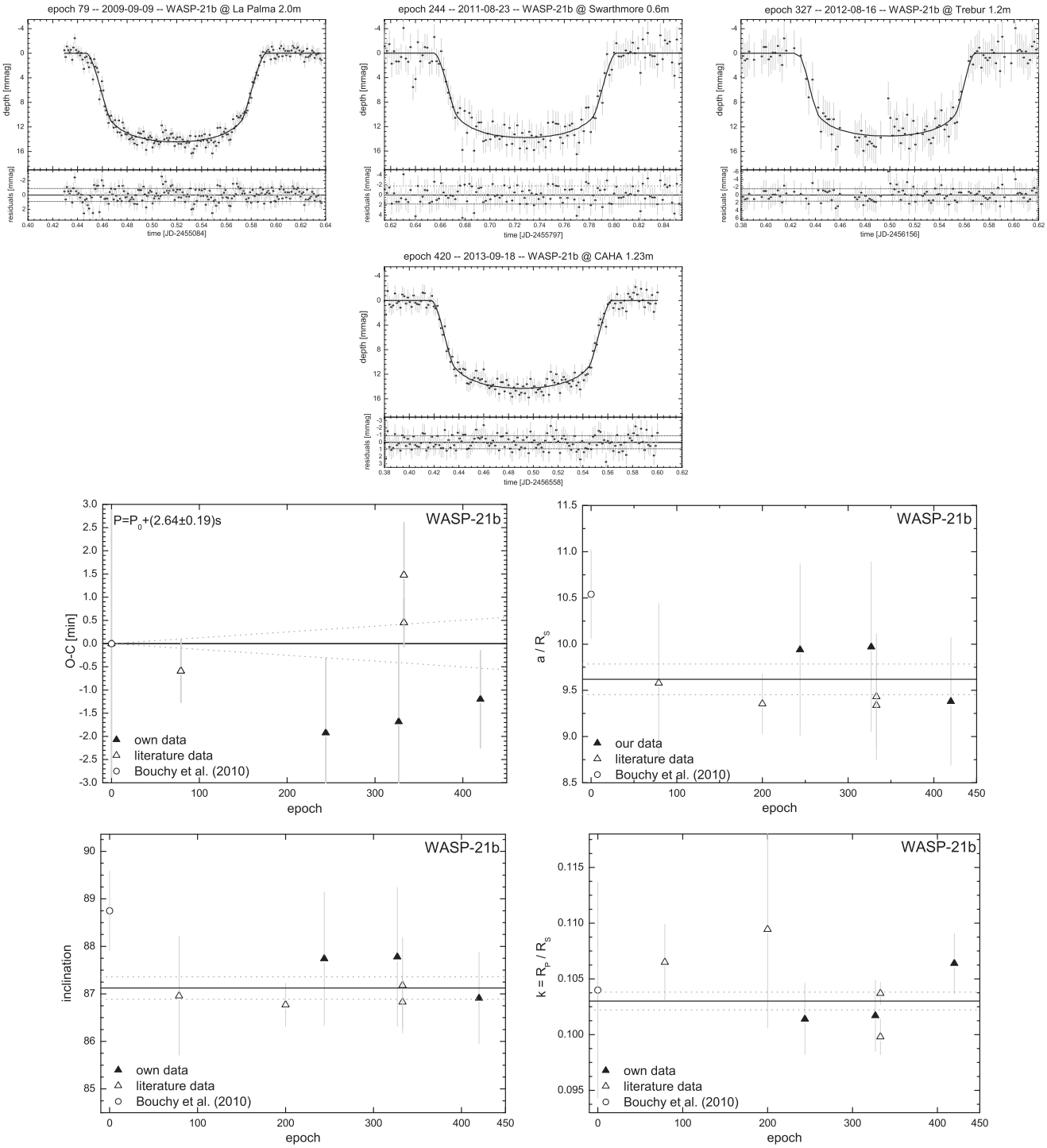

Figure 5. Top: the transit light curves obtained for WASP-21b. Bottom: the present result for the WASP-21b observing campaign. All explanations are equal to Fig. 2. The open circle denotes data from the discovery paper of Bouchy et al. (2010), open triangles denote literature data from Barros et al. (2011), Ciceri et al. (2013) and Southworth (2012) (the latter one artificially set to epoch 200), filled triangles denote our data (from Swarthmore, Trebur and Calar Alto).

as well as the weighted mean and the literature results. Though there are small deviations between the different transit events, no significant difference can be seen. Our observations point towards $b = 0.86$ and thus confirm the results of Anderson et al. (2011) and Béky et al. (2011). One has to state, though, that the error bars of the individual results are quite large. With $b > 0.8$ the HAT-P-27 system shows one of the largest known impact parameter of all known transiting exoplanets in combination with a very high probability that the transit is indeed gracing.

5.4 WASP-21b

Four transit light curves of WASP-21b are available, including one light curve from Barros et al. (2011) (see Fig. 5). In addition, the

Table 6. The results of the individual fits of the observed complete transit event. The rms of the fit and the resultant pnr are given in the last column. The table also shows the result for the transits with pnr > 4.5 that are not used for redetermining the system properties.

Date	Epoch	Telescope	$T_{\rm mid} - 245\,0000$ d	$a/R_{\rm s}$	$k = R_{\rm p}/R_{\rm s}$	i (°)	rms/pnr (mmag)
			HAT-P-18b				
2011-04-21	174	Trebur 1.2 m	5673.419 67 ± 0.001 24	16.4 ± 1.4	0.1399 ± 0.0072	88.52 ± 0.84	3.0 / 3.3
2011-05-24	180	Trebur 1.2 m	5706.469 93 ± 0.000 80	18.28 ± 0.83	0.1343 ± 0.0039	89.52 ± 0.58	3.7 / 4.0
2012-05-05	243	Rozhen 0.6 m	6053.472 76 ± 0.000 84	16.04 ± 1.36	0.1373 ± 0.0047	88.55 ± 0.79	3.5 / 4.4
2012-06-07	249	CA-DLR 1.2 m	6086.518 56 ± 0.001 25	–	–	–	4.1 / 4.5
2013-04-28	308	Antalya 1.0 m	6411.496 38 ± 0.000 84	15.22 ± 1.52	0.1464 ± 0.0068	87.89 ± 0.75	3.9 / 5.0
			HAT-P-19b				
2011-11-23	199	Jena 0.6 m	5899.283 45 ± 0.000 49	12.56 ± 0.34	0.1369 ± 0.0026	88.20 ± 0.64	2.1 / 2.2
2011-12-09	203	Jena 0.6 m	5905.318 10 ± 0.000 44	12.29 ± 0.35	0.1369 ± 0.0023	89.05 ± 0.67	2.3 / 2.4
2011-12-17	205	CA-DLR 1.2 m	5913.335 71 ± 0.000 34	11.96 ± 0.53	0.1368 ± 0.0027	88.38 ± 0.80	1.2 / 1.3
2014-10-04	460	Jena 0.6 m	6935.575 59 ± 0.000 55	12.43 ± 0.36	0.1340 ± 0.0026	89.25 ± 0.67	2.8 / 3.0
			HAT-P-27b				
2011-04-05	155	Lulin 0.4 m	5657.153 33 ± 0.001 07	10.72 ± 1.67	0.1233 ± 0.0081	85.53 ± 0.93	3.4 / 3.8
2011-04-08	156	Lulin 0.4 m	5660.194 81 ± 0.001 16	9.43 ± 1.01	0.1228 ± 0.0149	84.69 ± 0.81	3.4 / 3.2
2011-05-05	165	Trebur 1.2 m	5687.551 22 ± 0.000 51	9.83 ± 0.56	0.1153 ± 0.0029	85.07 ± 0.40	1.6 / 1.8
2012-04-01	274	Tenagra 0.8 m	6018.864 57 ± 0.002 32	9.65 ± 1.63	0.1199 ± 0.0126	84.13 ± 1.63	5.7 / 5.8
2012-04-25	282	Xinglong 0.6 m	6043.180 95 ± 0.001 35	9.89 ± 1.67	0.1186 ± 0.0067	84.83 ± 1.24	4.3 / 5.1
2013-06-03	415	Antalya 1.0 m	6447.442 68 ± 0.001 66	10.64 ± 1.30	0.1184 ± 0.0081	85.51 ± 0.94	2.6 / 3.5
2013-06-03	415	OSN 1.5 m	6447.445 71 ± 0.000 30	10.18 ± 0.29	0.1224 ± 0.0037	85.23 ± 0.21	1.2 / 0.9
2013-06-18	540	Antalya 1.0 m	6827.395 45 ± 0.002 20	10.77 ± 1.01	0.1462 ± 0.0141	85.26 ± 0.55	3.1 / 4.0
			WASP-21b				
2011-08-24	244	Swarthmore 0.6 m	5797.734 00 ± 0.001 12	9.94 ± 0.93	0.1014 ± 0.0032	87.74 ± 1.41	3.3 / 3.1
2012-08-16	327	Trebur 1.2 m	6156.502 60 ± 0.001 15	9.97 ± 0.92	0.1017 ± 0.0032	87.78 ± 1.46	2.9 / 2.6
2013-09-18	420	CA-DLR 1.2 m	6558.496 48 ± 0.000 73	9.38 ± 0.69	0.1064 ± 0.0027	86.91 ± 0.96	1.6 / 1.4

results of the analysis of two transit events of Ciceri et al. (2013) and one transit observation of Southworth (2012) are also taken into account. Concerning the O−C diagram, we found that a period change of (2.63 ± 0.17) s removes the linear trend which is present in the data fitted with the initial ephemeris. As in the previous analyses, no trend or sinusoidal variation in the system parameters can be seen.

However, regarding inclination and reverse fractional stellar radius we do see a significant difference between our results and the initial values published by Bouchy et al. (2010). This was also found by other authors before. As discussed in Barros et al. (2011), this result is a consequence of the assumption of Bouchy et al. (2010) that the planet host star is a main-sequence star, while Barros et al. (2011) found that the star starts evolving off the main sequence and thus its radius increases. This in turn leads to corrections of the stellar and hence planetary properties.

6 SUMMARY

We presented the results of the transit observations of the extrasolar planets HAT-P-18b, HAT-P-19b, HAT-P-27b/WASP-40b and WASP-21b which are part of our ongoing project on ground-based follow-up observations of exoplanetary transits using small- to medium-size telescopes with the help of YETI network telescopes. During the past three years we followed these well-chosen objects to refine their orbital parameters as well as to find TTVs indicating yet unknown planetary companions. Table 5 contains an overview of the redetermined properties, as well as the available literature values, while Table 6 lists the results of the individual light-curve fits.

In all cases we could redetermine the orbital parameters. Especially, the period could be determined more precise than before. So far, we cannot rule out the existence of TTV signals for the planets investigated within this study due to the limited number of available high-quality data. Also the parameters $a/R_{\rm s}$, $r_{\rm p}/r_{\rm s}$ and inclination have been obtained and compared to the available literature data. Despite some corrections to the literature data, we found no significant variations within these parameters. To distinguish between a real astrophysical source of the remaining scatter and random noise as a result of the quality of our data more high-precision transit observations would be needed.

HAT-P-18b was also part of an out-of-transit monitoring for a spread in the transit depth was reported in the literature that could be due to a significant variability of the transit host star. Regarding our transit data we cannot confirm the spread in transit depth. Looking at the quality of the literature data showing the transit depth variation, it is very likely that this spread is of artificial nature. Thus it is not surprising that we did not find stellar variability larger than ≈3.8 mmag. However, we do see some structures in the light curves that could be caused by spot activity on the stellar surface.

ACKNOWLEDGEMENTS

All the participating observatories appreciate the logistic and financial support of their institutions and in particular their technical workshops. MS would like to thank all participating YETI telescopes for their observations, as well as G. Maciejewski and the anonymous referee for helpful comments on this work. JGS, AP, and RN would like to thank the Deutsche Forschungsgemeinschaft (DFG) for support in the Collaborative Research Center Sonderforschungsbereich SFB TR 7 'Gravitationswellenastronomie'. RE, MK, SR and RN would like to thank the DFG for support in the Priority Programme SPP 1385 on the First ten Million years of the Solar system in projects NE 515/34-1 and -2. RN would like to

acknowledge financial support from the Thuringian government (B 515-07010) for the STK CCD camera (Jena 0.6 m) used in this project. MM and CG thank DFG in project MU 2695/13-1. The research of DD and DK was supported partly by funds of projects DO 02-362, DO 02-85 and DDVU 02/40-2010 of the Bulgarian Scientific Foundation, as well as project RD-08-261 of Shumen University. Z-YU was supported by the Chinese National Natural Science Foundation grant no. 11373033. The research of RC, MH and MH is supported as a project of the Nordrhein-Westfälische Akademie der Wissenschaften und Künste in the framework of the academy programme by the Federal Republic of Germany and the state Nordrhein-Westfalen. MF acknowledges financial support from grants AYA2011-30147-C03-01 of the Spanish Ministry of Economy and Competitiveness (MINECO), cofunded with EU FEDER funds, and 2011 FQM 7363 of the Consejería de Economía, Innovación, Ciencia y Empleo (Junta de Andalucía, Spain). We also wish to thank the TÜBİTAK National Observatory (TUG) for supporting this work through project numbers 12BT100-324-0 and 12CT100-388 using the T100 telescope. MS thanks D. Keeley, M. M. Hohle and H. Gilbert for supporting the observations at the University Observatory Jena. This research has made use of NASA's Astrophysics Data System. This research is based on observations obtained with telescopes of the University Observatory Jena, which is operated by the Astrophysical Institute of the Friedrich-Schiller-University. This work has been supported in part by Istanbul University under project number 39742, by a VEGA Grant 2/0143/14 of the Slovak Academy of Sciences and by the joint fund of Astronomy of the National Science Foundation of China and the Chinese Academy of Science under grants U1231113.

REFERENCES

Anderson D. R. et al., 2011, PASP, 123, 555
Bakos G., Noyes R. W., Kovács G., Stanek K. Z., Sasselov D. D., Domsa I., 2004, PASP, 116, 266
Barros S. C. C., Pollacco D. L., Gibson N. P., Howarth I. D., Keenan F. P., Simpson E. K., Skillen I., Steele I. A., 2011, MNRAS, 416, 2593
Barros S. C. C. et al., 2014, A&A, 561, L1
Béky B. et al., 2011, ApJ, 734, 109
Borucki W. J. et al., 2011, ApJ, 728, 117
Bouchy F. et al., 2010, A&A, 519, A98
Broeg C., Fernández M., Neuhäuser R., 2005, Astron. Nachr., 326, 134
Brown D. J. A. et al., 2012, ApJ, 760, 139
Carter J. A., Winn J. N., 2009, ApJ, 704, 51
Ciceri S. et al., 2013, A&A, 557, A30
Claret A., Bloemen S., 2011, A&A, 529, A75
Eastman J., Siverd R., Gaudi B. S., 2010, PASP, 122, 935
Eastman J., Gaudi B. S., Agol E., 2013, PASP, 125, 83
Esposito M. et al., 2014, A&A, 564, L13
Etzel P. B., 1981, in Carling E. B., Kopal Z., eds, Proc. NATO ASI, Photometric and Spectroscopic Binary Systems. Reidel, Dordrecht, p. 111
Ford E. B., Holman M. J., 2007, ApJ, 664, L51
Fulton B. J., Shporer A., Winn J. N., Holman M. J., Pál A., Gazak J. Z., 2011, AJ, 142, 84
Gazak J. Z., Johnson J. A., Tonry J., Dragomir D., Eastman J., Mann A. W., Agol E., 2012, Adv. Astron., 2012, 30
Ginski C., Mugrauer M., Seeliger M., Eisenbeiss T., 2012, MNRAS, 421, 2498
Hartman J. D. et al., 2011, ApJ, 726, 52
Knutson H. A. et al., 2014, ApJ, 785, 126
Koch D. G. et al., 2010, ApJ, 713, L79
Maciejewski G. et al., 2010, MNRAS, 407, 2625
Maciejewski G. et al., 2011a, MNRAS, 411, 1204
Maciejewski G., Errmann R., Raetz St., Seeliger M., Spaleniak I., Neuhäuser R., 2011b, A&A, 528, A65
Maciejewski G. et al., 2013a, AJ, 146, 147
Maciejewski G. et al., 2013b, A&A, 551, A108
Mandel K., Agol E., 2002, ApJ, 580, L171
Mazeh T. et al., 2013, ApJS, 208, 16
Mugrauer M., Berthold T., 2010, Astron. Nachr., 331, 449
Nesvorný D., Kipping D., Terrell D., Hartman J., Bakos G. Á., Buchhave L. A., 2013, ApJ, 777, 3
Neuhäuser R. et al., 2011, Astron. Nachr., 332, 547
Poddaný S., Brát L., Pejcha O., 2010, New Astron., 15, 297
Pollacco D. L. et al., 2006, PASP, 118, 1407
Popper D. M., Etzel P. B., 1981, AJ, 86, 102
Raetz St., 2012, PhD thesis, University Jena
Raetz St. et al., 2014, MNRAS, 444, 1351
Raetz St. et al., 2015, MNRAS, 000, 00
Sada P. V. et al., 2012, PASP, 124, 212
Seeliger M. et al., 2014, MNRAS, 441, 304
Simpson E. K. et al., 2010, MNRAS, 405, 1867
Smalley B. et al., 2011, A&A, 526, A130
Southworth J., 2008, MNRAS, 386, 1644
Southworth J., 2012, MNRAS, 426, 1291
Southworth J. et al., 2009a, MNRAS, 396, 1023
Southworth J. et al., 2009b, MNRAS, 399, 287
Steffen J. H. et al., 2012, PNAS, 109, 7982
Szabó R., Szabó G. M., Dálya G., Simon A. E., Hodosán G., Kiss L. L., 2013, A&A, 553, A17
von Essen C., Schröter S., Agol E., Schmitt J. H. M. M., 2013, A&A, 555, A92
Winn J. N., 2010, preprint (arXiv:1001.2010)

[1]*Astrophysical Institute and University Observatory Jena, Schillergäßchen 2-3, D-07745 Jena, Germany*
[2]*Abbe Center of Photonics, Friedrich Schiller Universität, Max-Wien-Platz 1, D-07743 Jena, Germany*
[3]*Astronomie Stiftung Trebur, Michael Adrian Observatorium, Fichtenstraße 7, D-65468 Trebur, Germany*
[4]*University of Applied Sciences, Technische Hochschule Mittelhessen, D-61169 Friedberg, Germany*
[5]*Graduate Institute of Astronomy, National Central University, Jhongli City, Taoyuan County 32001, Taiwan, Republic of China*
[6]*Sabanci University, Orhanli-Tuzla 34956, Istanbul, Turkey*
[7]*Department of Astronomy and Space Sciences, Faculty of Sciences, Istanbul University, 34119 İstanbul, Turkey*
[8]*Deutsches Zentrum für Luft- und Raumfahrt e.V., Institut für Planetenforschung, Rutherfordstr. 2, D-12489 Berlin, Germany*
[9]*Instituto de Astrofisica de Andalucia, CSIC, Apdo. 3004, E-18080 Granada, Spain*
[10]*Institute of Astronomy and NAO, Bulgarian Academy of Sciences, 72 Tsarigradsko Chaussee Blvd, 1784 Sofia, Bulgaria*
[11]*Shumen University, 115 Universitetska str., 9700 Shumen, Bulgaria*
[12]*Department of Physics and Astronomy, Swarthmore College, Swarthmore, PA 19081, USA*
[13]*Astronomical Institute, Slovak Academy of Sciences, 059 60 Tatranská Lomnica, Slovakia*
[14]*Research School of Astronomy and Astrophysics, Australian National University, Canberra, ACT 2611, Australia*
[15]*Leibnitz-Institut für Astrophysik Potsdam, An der Sternwarte 16, D-14482 Potsdam, Germany*
[16]*Key Laboratory of Optical Astronomy, NAO, Chinese Academy of Sciences, 20A Datun Road, Beijing 100012, China*
[17]*European Space Agency, ESTEC, SRE-S, Keplerlaan 1, NL-2201 AZ Noordwijk, the Netherlands*
[18]*Hamburger Sternwarte, Gojenbergsweg 112, D-21029 Hamburg, Germany*
[19]*Gettysburg College Observatory, Department of Physics, 300 North Washington St, Gettysburg, PA 17325, USA*

[20] *Astronomisches Institut, Ruhr-Universität Bochum, Universitätsstraße 150, D-44780 Bochum, Germany*
[21] *Instituto de Astronomía, Universidad Católica del Norte, Avenida Angamos 0610, Casilla 1280 Antofagasta, Chile*
[22] *Department of Astronomy and Space Sciences, Faculty of Science, University of Ege, Bornova, 35100 İzmir, Turkey*
[23] *Graduate School of Science and Engineering, Department of Astronomy and Space Sciences, Istanbul University, 34116 Istanbul, Turkey*
[24] *Sterrewacht Leiden, PO Box 9513, Niels Bohrweg 2, NL-2300 RA Leiden, the Netherlands*
[25] *Centre for Astronomy, Faculty of Physics, Astronomy and Informatics, N. Copernicus University, Grudziadzka 5, PL-87-100 Toruń, Poland*

This paper has been typeset from a TEX/LATEX file prepared by the author.